

AD-A114 149

MASSACHUSETTS INST OF TECH LEXINGTON LINCOLN LAB F/8 9/5
ACOUSTOOPTIC TIME-INTEGRATING CORRELATORS AND OPTOELECTRONIC MI--ETC(U)
JAN 82 A 6 FOYT, R C WILLIAMSON F19628-80-C-0002

UNCLASSIFIED

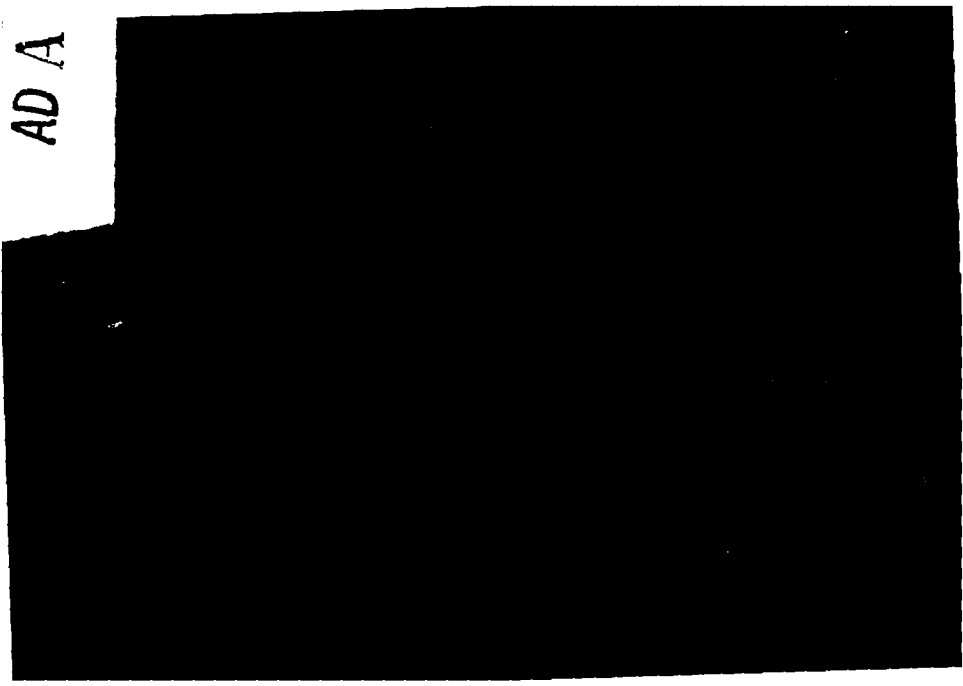
ESD-TR-82-008

NL

End
Product

END
DATE
FILMED
5-82
DTIC

AD A



MASSACHUSETTS INSTITUTE OF TECHNOLOGY
LINCOLN LABORATORY

**ACOUSTOOPTIC TIME-INTEGRATING CORRELATORS
AND OPTOELECTRONIC MIXERS**

**ANNUAL REPORT
TO THE
AIR FORCE OFFICE OF SCIENTIFIC RESEARCH
ELECTRONICS AND SOLID STATE SCIENCES DIVISION**

*A.G. FOYT
R.C. WILLIAMSON
Co-Principal Investigators
Group 85*

1 FEBRUARY 1981 — 31 JANUARY 1982

ISSUED 11 MARCH 1982

Approved for public release; distribution unlimited.

LEXINGTON

MASSACHUSETTS

1. ABSTRACT

Research during the past year has been concentrated on the development of the InP optoelectronic switch and on the evaluation of this switch as an electronic mixer. This type of mixer appears well suited for use in a time-integrating correlator which employs a heterodyne detector array. In such an array, a small high-quality mixer is crucial.

InP optoelectronic switches have been fabricated using interdigitated-finger electrode structures with finger and space lengths varying from 6 μm for the most widely spaced device to 1.25 μm for the most closely spaced device and active areas of 48 x 48 μm . Devices fabricated using alloyed Au/Ge/Ni contacts have shown near-theoretical conductance when illuminated with laser light from either a He-Ne laser ($\lambda \sim 0.63 \mu\text{m}$) or from a AlGaAs laser ($\lambda \sim 0.84 \mu\text{m}$). For a device with 1.25- μm lines and spaces and with a 3-nsec photoconductor response fall time, an on-state (illuminated) resistance value of <18 ohms was measured using 6 mW of AlGaAs diode laser light power. Also, these devices exhibit a linear variation of on-state conductance with laser intensity from low light levels to levels greater than 2 mW. Such linear variation is essential for the operation of the device as a bilinear mixer. Finally, it has been found that the response times of these devices are somewhat dependent on the starting material, with the photoresponse fall times (90% to 10% of peak response) varying from ~ 6 nsec to 0.5 nsec. Also, it has been shown that proton bombardment can dramatically reduce the response time with only a modest change in the amplitude of the response. The 90%-to-10% fall time of a device with an initial fall time of 5 nsec was reduced to ~ 100 psec following a 200-kV $10^{13}/\text{cm}^2$ proton bombardment and subsequent anneal at 250°C, with the amplitude of the response

The performance of these devices in both the conventional (switch) mode and the bilinear mode of mixing has been evaluated. For a structure with 2- μm lines and spaces and a photoresponse fall time of ~ 3 nsec, illumination with ~ 5 mW of AlGaAs laser power resulted in an on-state resistance of 21 ohms. For this device operating in the switch mode at 1 MHz, the third-order two-tone intermodulation products were -55 dBm for ~ 0 dBm of rf input power. A simple extrapolation suggests that these products could be lowered to -85 dBm at the same rf power level by reducing the on-state resistance by one-half which reduction should be possible to do by reducing the finger and space dimension, by reducing the intercept resistance, or by increasing the laser power. In a preliminary investigation of the bilinear mode of operation at 1 MHz, the multiplied output varied linearly with the rf input to the switch over a 20-dB range and with the input to the diode laser, also over at least a 20-dB range.

Association For
 1961 ☒
 1962 ☐
 1963 ☐
 1964 ☐
 1965 ☐
 1966 ☐
 1967 ☐
 1968 ☐
 1969 ☐
 1970 ☐
 1971 ☐
 1972 ☐
 1973 ☐
 1974 ☐
 1975 ☐
 1976 ☐
 1977 ☐
 1978 ☐
 1979 ☐
 1980 ☐
 1981 ☐
 1982 ☐
 1983 ☐
 1984 ☐
 1985 ☐
 1986 ☐
 1987 ☐
 1988 ☐
 1989 ☐
 1990 ☐
 1991 ☐
 1992 ☐
 1993 ☐
 1994 ☐
 1995 ☐
 1996 ☐
 1997 ☐
 1998 ☐
 1999 ☐
 2000 ☐
 2001 ☐
 2002 ☐
 2003 ☐
 2004 ☐
 2005 ☐
 2006 ☐
 2007 ☐
 2008 ☐
 2009 ☐
 2010 ☐
 2011 ☐
 2012 ☐
 2013 ☐
 2014 ☐
 2015 ☐
 2016 ☐
 2017 ☐
 2018 ☐
 2019 ☐
 2020 ☐
 2021 ☐
 2022 ☐
 2023 ☐
 2024 ☐
 2025 ☐
 2026 ☐
 2027 ☐
 2028 ☐
 2029 ☐
 2030 ☐
 2031 ☐
 2032 ☐
 2033 ☐
 2034 ☐
 2035 ☐
 2036 ☐
 2037 ☐
 2038 ☐
 2039 ☐
 2040 ☐
 2041 ☐
 2042 ☐
 2043 ☐
 2044 ☐
 2045 ☐
 2046 ☐
 2047 ☐
 2048 ☐
 2049 ☐
 2050 ☐
 2051 ☐
 2052 ☐
 2053 ☐
 2054 ☐
 2055 ☐
 2056 ☐
 2057 ☐
 2058 ☐
 2059 ☐
 2060 ☐
 2061 ☐
 2062 ☐
 2063 ☐
 2064 ☐
 2065 ☐
 2066 ☐
 2067 ☐
 2068 ☐
 2069 ☐
 2070 ☐
 2071 ☐
 2072 ☐
 2073 ☐
 2074 ☐
 2075 ☐
 2076 ☐
 2077 ☐
 2078 ☐
 2079 ☐
 2080 ☐
 2081 ☐
 2082 ☐
 2083 ☐
 2084 ☐
 2085 ☐
 2086 ☐
 2087 ☐
 2088 ☐
 2089 ☐
 2090 ☐
 2091 ☐
 2092 ☐
 2093 ☐
 2094 ☐
 2095 ☐
 2096 ☐
 2097 ☐
 2098 ☐
 2099 ☐
 2100 ☐
 2101 ☐
 2102 ☐
 2103 ☐
 2104 ☐
 2105 ☐
 2106 ☐
 2107 ☐
 2108 ☐
 2109 ☐
 2110 ☐
 2111 ☐
 2112 ☐
 2113 ☐
 2114 ☐
 2115 ☐
 2116 ☐
 2117 ☐
 2118 ☐
 2119 ☐
 2120 ☐
 2121 ☐
 2122 ☐
 2123 ☐
 2124 ☐
 2125 ☐
 2126 ☐
 2127 ☐
 2128 ☐
 2129 ☐
 2130 ☐
 2131 ☐
 2132 ☐
 2133 ☐
 2134 ☐
 2135 ☐
 2136 ☐
 2137 ☐
 2138 ☐
 2139 ☐
 2140 ☐
 2141 ☐
 2142 ☐
 2143 ☐
 2144 ☐
 2145 ☐
 2146 ☐
 2147 ☐
 2148 ☐
 2149 ☐
 2150 ☐
 2151 ☐
 2152 ☐
 2153 ☐
 2154 ☐
 2155 ☐
 2156 ☐
 2157 ☐
 2158 ☐
 2159 ☐
 2160 ☐
 2161 ☐
 2162 ☐
 2163 ☐
 2164 ☐
 2165 ☐
 2166 ☐
 2167 ☐
 2168 ☐
 2169 ☐
 2170 ☐
 2171 ☐
 2172 ☐
 2173 ☐
 2174 ☐
 2175 ☐
 2176 ☐
 2177 ☐
 2178 ☐
 2179 ☐
 2180 ☐
 2181 ☐
 2182 ☐
 2183 ☐
 2184 ☐
 2185 ☐
 2186 ☐
 2187 ☐
 2188 ☐
 2189 ☐
 2190 ☐
 2191 ☐
 2192 ☐
 2193 ☐
 2194 ☐
 2195 ☐
 2196 ☐
 2197 ☐
 2198 ☐
 2199 ☐
 2200 ☐
 2201 ☐
 2202 ☐
 2203 ☐
 2204 ☐
 2205 ☐
 2206 ☐
 2207 ☐
 2208 ☐
 2209 ☐
 2210 ☐
 2211 ☐
 2212 ☐
 2213 ☐
 2214 ☐
 2215 ☐
 2216 ☐
 2217 ☐
 2218 ☐
 2219 ☐
 2220 ☐
 2221 ☐
 2222 ☐
 2223 ☐
 2224 ☐
 2225 ☐
 2226 ☐
 2227 ☐
 2228 ☐
 2229 ☐
 2230 ☐
 2231 ☐
 2232 ☐
 2233 <

DTIC
COPY
INSPECTED
2

CONTENTS

Abstract	111
Publications and Meeting Speeches	vi
I. Introduction	1
II. InP Optoelectronic Mixer Development	2
1. On-state Resistance	2
2. Linear Conductance	10
3. Response Time	10
III. Mixer Results	21
1. Switch Mode	21
2. Bilinear Mode	24
IV. Professional Personnel	26

PUBLICATIONS

1. A. G. Foyt, F. J. Leonberger and R. C. Williamson, "InP Optoelectronic Mixers," Proc. SPIE, Vol. 269: Integrated Optics, 1981, p. 109.
2. A. G. Foyt, F. J. Leonberger and R. C. Williamson, "InP Optoelectronic Mixers," IEEE Trans. Electron Devices ED-28, 1214 (1981).
3. A. G. Foyt, F. J. Leonberger and R. C. Williamson "Picosecond InP Optoelectronic Switches," Appl. Phys. Lett. (accepted for publication).

MEETING SPEECHES

1. A. G. Foyt, F. J. Leonberger and R. C. Williamson, "InP Optoelectronic Mixers," SPIE Los Angeles, CA, 9-13 February, 1981.
2. A. G. Foyt, F. J. Leonberger and R. C. Williamson, "InP Optoelectronic Mixers," IEEE Device Research Conf., Santa Barbara, CA, 22-24 June, 1981.
3. A. G. Foyt, F. J. Leonberger and R. C. Williamson, "Picosecond InP Optoelectronic Switches," accepted for presentation at CLEO'82, Phoenix, AZ, 14-16 April, 1982.

I. INTRODUCTION

InP optoelectronic switches are potentially useful as high-speed electronic mixers and samplers. For such applications, the advantages of these devices include linearity, lack of a dc offset, and isolation of the local oscillator drive signal from the output. These features should make this device attractive for such applications as synchronous detection and bilinear mixing, as well as for high-speed sampling. Also, these devices may be useful in optical signal processing applications such as Time-Integrating Correlators. Prior to the start of the present program, the development of these InP devices had included the fabrication of structures with simple gaps in the metalization and the evaluation of these devices in sampling and pulse-generation applications.* Also, an interdigitated-finger electrode structure was developed and the use of Au/Sn alloyed metal contacts was investigated in order to increase the device on-state (illuminated) conductance.** Also, a preliminary investigation of the use of this device as a synchronous demodulator was investigated.**

During the past year (the first year of this program), further development of the interdigitated structure and the use of alloyed Au/Ge/Ni contacts has resulted in near-theoretical values of on-state conductance. Also, the conductance has been shown to be linearly related to the light intensity over at least four orders of magnitude, a feature important for some mixing applications. Also, the response times of these devices have been shown to depend on the starting material with 90-to-10% photoresponse fall times ranging from

*F. J. Leonberger and P. F. Moulton, Appl. Phys. Lett. 35, 712 (1979).

**A. G. Foyt, F. J. Leonberger and R. C. Williamson, Proc. SPIE, Vol. 269: Integrated Optics, 1981, p. 109.

6 to 0.5 nsec. Proton bombardment has been used to further reduce the response time, and values <100 psec have been measured. Also, during the past year, the use of these devices as mixers has been further evaluated, both in the conventional (switch) mode as well as in a bilinear mode. For the switch mode, these measurements indicate that the InP devices should be competitive with diode-bridge mixers.

In this report, the development of the InP optoelectronic devices will be presented first, and the evaluation of these devices as mixers discussed subsequently.

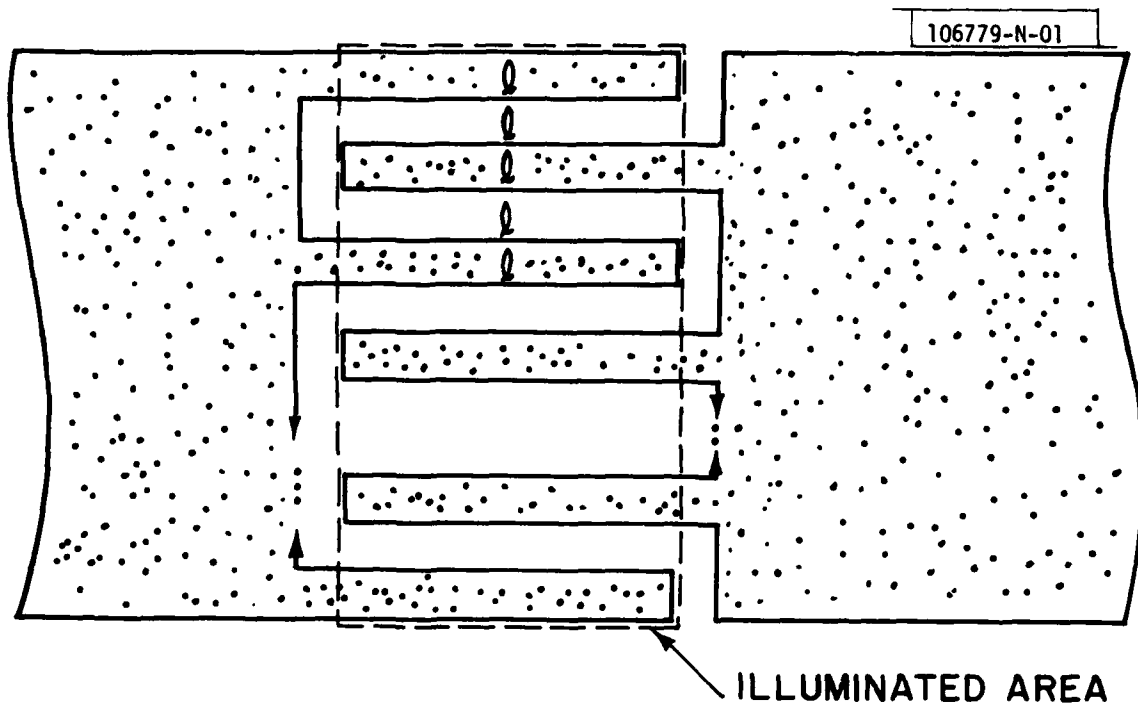
II. InP OPTOELECTRONIC MIXER DEVELOPMENT

1. On-state Resistance

Prior to the present program, both simple gap-structure and interdigitated-finger-electrode-structure InP optoelectronic switches had been investigated. It is straightforward to show that the interdigitated structure offers lower on-state resistance as the size of the gap in the simple gap structure becomes smaller than the size of the light spot that illuminates the gap. If the light spot just fills the finger and space area of an interdigitated structure, as shown in Fig. 1, then the on-state (illuminated) resistance for a constant light level is, assuming uniform current flow and no contact resistance,

$$R = \frac{1}{P\tau\mu} \frac{h\nu}{e} \ell^2 \quad (1)$$

where ℓ is the finger and space length, P is the absorbed optical power, $h\nu$ is the photon energy, e the electronic charge, τ the photoconductive lifetime and μ the carrier mobility. In this calculation, the absorbed optical power is related to the incident power by



$$R_{ON} \sim \frac{l^2}{P} \quad C_{OFF} \sim A/l$$

$$\omega_C = (R_{ON} C_{OFF})^{-1} \sim P/lA$$

Fig. 1. Sketch of an interdigitated-finger-structure optoelectronic mixer. The relationships of the on-state resistance R_{ON} , the off-state capacitance C_{OFF} and the cutoff frequency ω_C to the finger width l , illuminated area A and total light power P are shown.

$$P_{\text{absorbed}} = \frac{1}{2} (1-R) P_{\text{incident}} \quad (2)$$

where R is the reflectivity of the InP and the 1/2 factor accounts for the light incident on the metal electrodes. Also, it has been assumed that each absorbed photon creates one hole-electron pair in the InP. For applications in which the on-state resistance must be minimized, a small finger length is clearly desirable. Also, high mobility and long carrier lifetime yield low on-state resistance. InP is well suited for optoelectronic switch applications because the material has an attractively high mobility.

Prior to the present program, interdigital-electrode structures with finger lengths of 6, 4 and 2 μm had been fabricated with both Ti/Au and Au/Sn metalizations. The Ti/Au system was investigated because it is a standard contact metalization, with the Ti used as an adhering layer to the InP and the Au as a bonding metal. The Au/Sn system, however, was used to investigate the possibility that an alloyed n-type contact would provide a lower on-state resistance, since the higher-mobility electrons were expected to provide most of the photoconductivity. The results for this system are shown in Fig. 2. In this experiment, a He-Ne laser was used as the light source, and the power incident on the finger structure was ~ 1 mW. As shown, the unalloyed (unannealed) devices did have a λ^2 dependence of the on-state resistance. However, the resistance extrapolated to zero gap (intercept resistance) was large (>1000 ohms). Similar results were seen for the Ti/Au samples. By heating the samples in various cycles, lower intercept resistances were seen. The anneal at 325°C for 12 hours gave the best result, with an intercept resistance of 200 ohms. Subsequent longer time and/or higher temperature anneals gave higher intercept resistances. In a subsequent

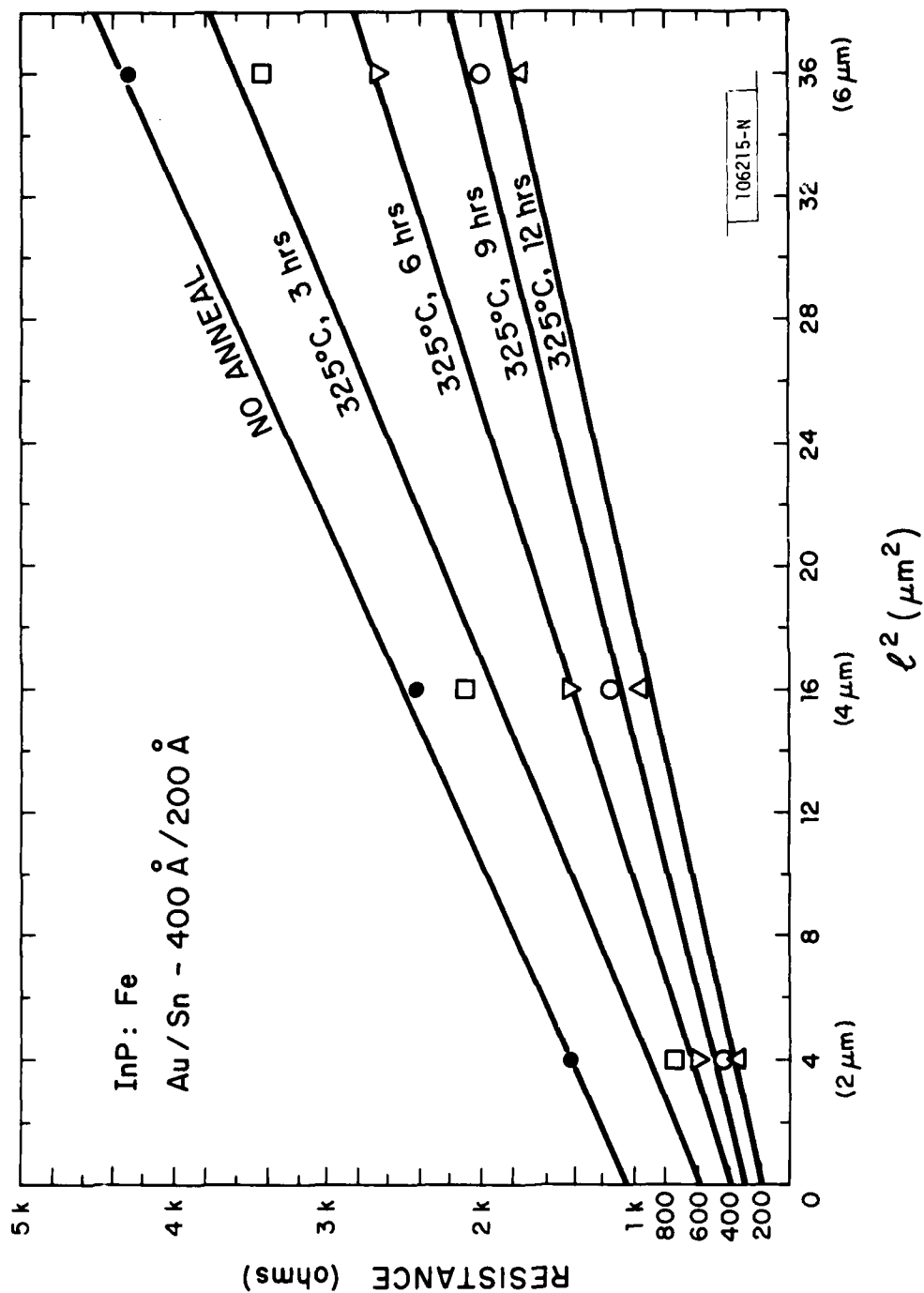


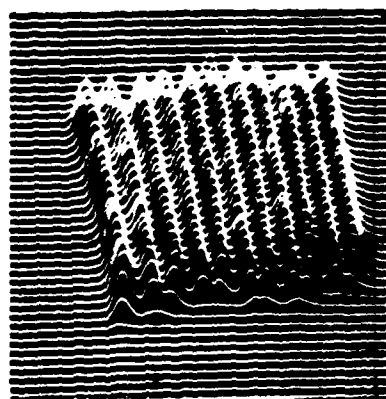
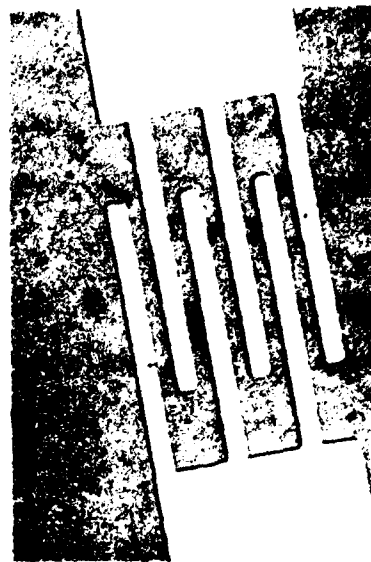
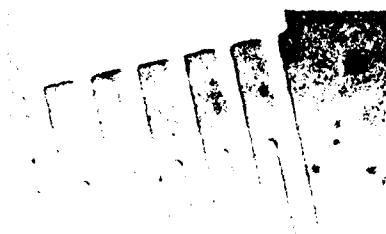
Fig. 2. Resistance vs length for Fe-doped InP optoelectronic mixers with Au:Sn contacts, after fabrication and after several subsequent annealing cycles. The resistance shown is in response to a 1-mW He-Ne ($\lambda \sim 0.63 \mu m$) laser spot uniformly illuminating the finger structure.

discussion of other contact materials, it will be shown that the intercept resistance is dependent on the optical power level, and that the usual interpretation of this quantity as a contact resistance must be used with caution.

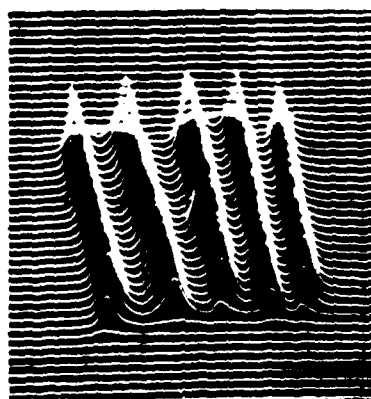
During the first year of this program, smaller geometry devices have been developed in an effort to minimize the device on-state resistance. Structures with finger and space lengths as small as $1.25\text{ }\mu\text{m}$ can now be fabricated. Also, improved contact metalization techniques have been investigated to minimize this resistance. The best results have been achieved using the following process. First, the etched InP slices are coated with Shipley AZ1450J photoresist. Conformable-mask lithography is then used to pattern the samples, and a brief chlorobenzene soak is used to provide a slight lip on the photoresist. The metals are then evaporated onto the samples in an electron-beam oil-diffusion-pump system. An evaporation sequence of Ni (400 Å) then Ge (300 Å), and finally Au (3400 Å) was used. The samples are then removed from the evaporator, and the excess metal removed in the lift-off process. The top surface of each sample is then covered with a 2000-Å layer of pyrolytic phosphosilicate glass (PSG) deposited at 250°C , and the sample is heated to 450°C for ten seconds to alloy the contacts. The PSG is then removed, and the samples are ready for subsequent evaluation.

Preliminary measurements were done using a system in which the light from a HeNe laser ($\lambda \sim 0.633\text{ }\mu\text{m}$) was focussed and raster scanned across the device. A dc bias was applied to one side of the device, and the other side connected to an oscilloscope on which the response was displayed in synchronism with the raster scan, in order to investigate the uniformity of response of these devices. The results for two structures are shown in Fig. 3, where it is clear that a uniform response is obtained.

C85-3578



2 μm lines



4 μm lines

Fig. 3. Response scans of a 4- and a 2- μm interdigitated-finger InP optoelectronic mixer using a scanned He-Ne ($\lambda \sim 0.63 \mu\text{m}$) laser spot. The laser power was $\sim 1 \text{ mW}$.

The variation of the on-state resistance as a function of finger length was measured by defocussing the HeNe laser light until it just covered the finger area on a device, and measuring the resulting resistance for several devices, all at a fixed light level of 1 mW. The results for two groups of devices with the Au/Ge/Ni metalization are shown in Fig. 4, along with the best result for the (earlier) Au/Sn metalized devices. All three groups of devices have a l^2 dependence of the on-state resistance, as expected.

One unexpected result shown in Fig. 4 is the fact that, in each case, the l^2 extrapolation to zero length yields a finite value, which we define as an intercept resistance. This effect is similar to that observed for metallic contacts to doped semiconductors, except that in this case, the carriers in the conducting region are photogenerated. It should be noted that this intercept resistance must also be a function of light level, because a 1.25- μ m device had an on-state resistance of ~ 18 ohms in response to 6 mW of power from an AlGaAs diode laser. The Au/Ge/Ni devices clearly have much lower values of resistance, and are superior devices. Even for these devices, there is still some intercept resistance, and the reduction of this resistance would result in still better performance. It is clear that until this intercept resistance is reduced, there is little advantage in a further reduction in finger dimension. For comparison, a calculated R vs l^2 line is also shown in Fig. 4, which line was computed using Eq. (1) and the values $\mu = 2000 \text{ cm}^2/\text{V-sec}$ and $\tau = 2 \text{ nsec}$. These are typical values for the bulk electron mobility and photoconductive lifetime of these samples. Equation (1) assumes that the current flows uniformly throughout the conducting region. However, it is clear that in these devices with surface interdigital electrodes, the current is nonuniform with a high-field region and a current-crowding effect near the edge of each electrode. This effect may account for the observed intercept resistance.

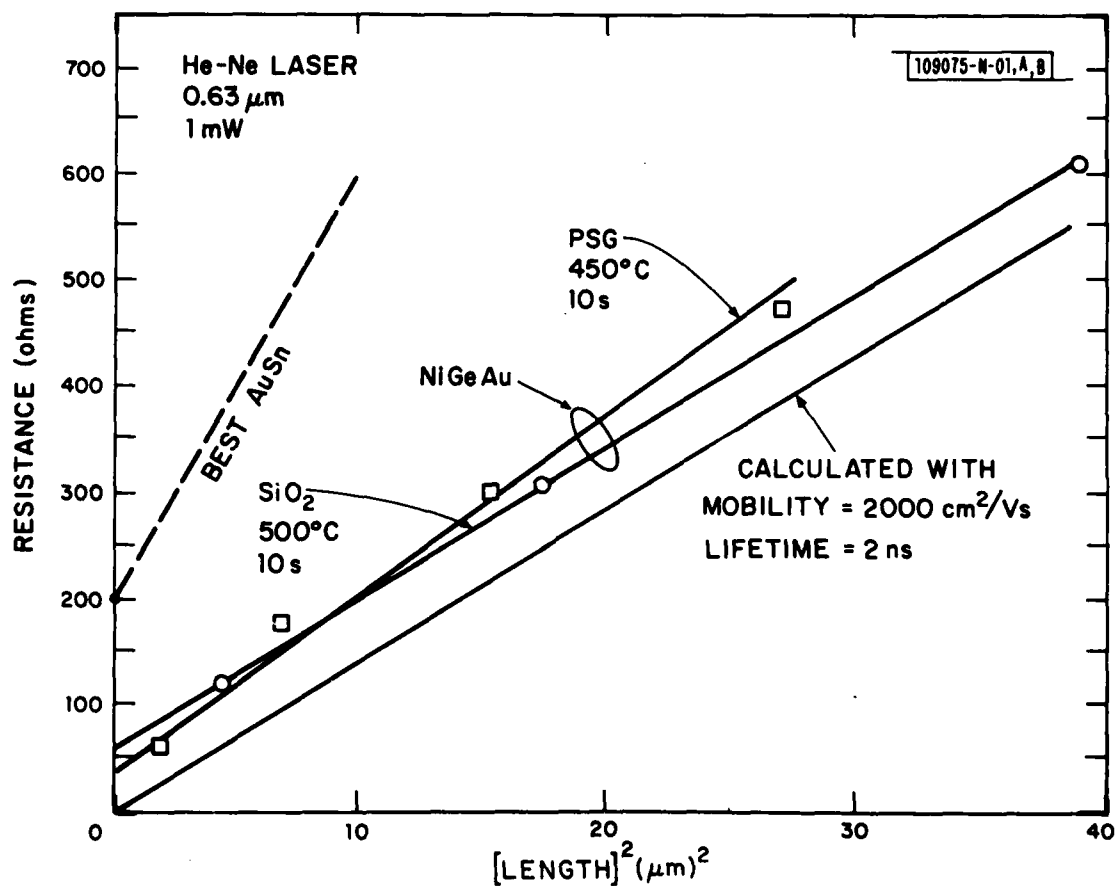


Fig. 4. Resistance vs length for Fe-doped InP optoelectronic mixers with NiGeAu contacts, after fabrication and after several subsequent alloying cycles. The resistance shown is in response to a 1-mW He-Ne ($\lambda \sim 0.63 \mu\text{m}$) laser spot uniformly illuminating the finger structure. The results of the best Au:Sn contact results are shown for comparison.

2. Linear Conductance

For applications in which the InP optoelectronic mixer is operated in the switch mode, the achievement of a low on-state resistance is important to low-insertion-loss, switch operation with good rf linearity. However, for other applications in which the desired output is linear in both mixer inputs, it is important for the device to have linear properties. As will be discussed more fully in a later section, one such property is the linearity of device conductance with light intensity. Figure 5 shows the measured conductance as a function of light intensity for one of the Au/Ge/Ni devices. There is a linear relation between conductance and light intensity over several orders of magnitude, extending from low light levels to power of a few mW. At higher light levels, there appears to be a tendency toward saturation. It is interesting to note that this linear relation is obtained for resistance levels comparable to the intercept resistance values seen in Fig. 4 for optical power levels of 1 mW. This result suggests that the quantity, $(\text{intercept resistance})^{-1}$, is linear in the optical power level.

3. Response Time

The maximum frequency ω_m of variation in light intensity to which a photoconductor will respond is limited by the photoconductive lifetime τ , where $\omega_m = (\tau)^{-1}$. It is therefore possible to define a figure of merit given by the conductivity-bandwidth product:

$$R^{-1} \omega_m = \frac{P_{\mu e}}{h\nu \ell^2} \quad (3)$$

The only material parameter in this figure of merit is the mobility.

In the off-state, the impedance is dominated by the capacitance which is

$$C = \frac{A}{4\ell} \hat{C} \quad (4)$$

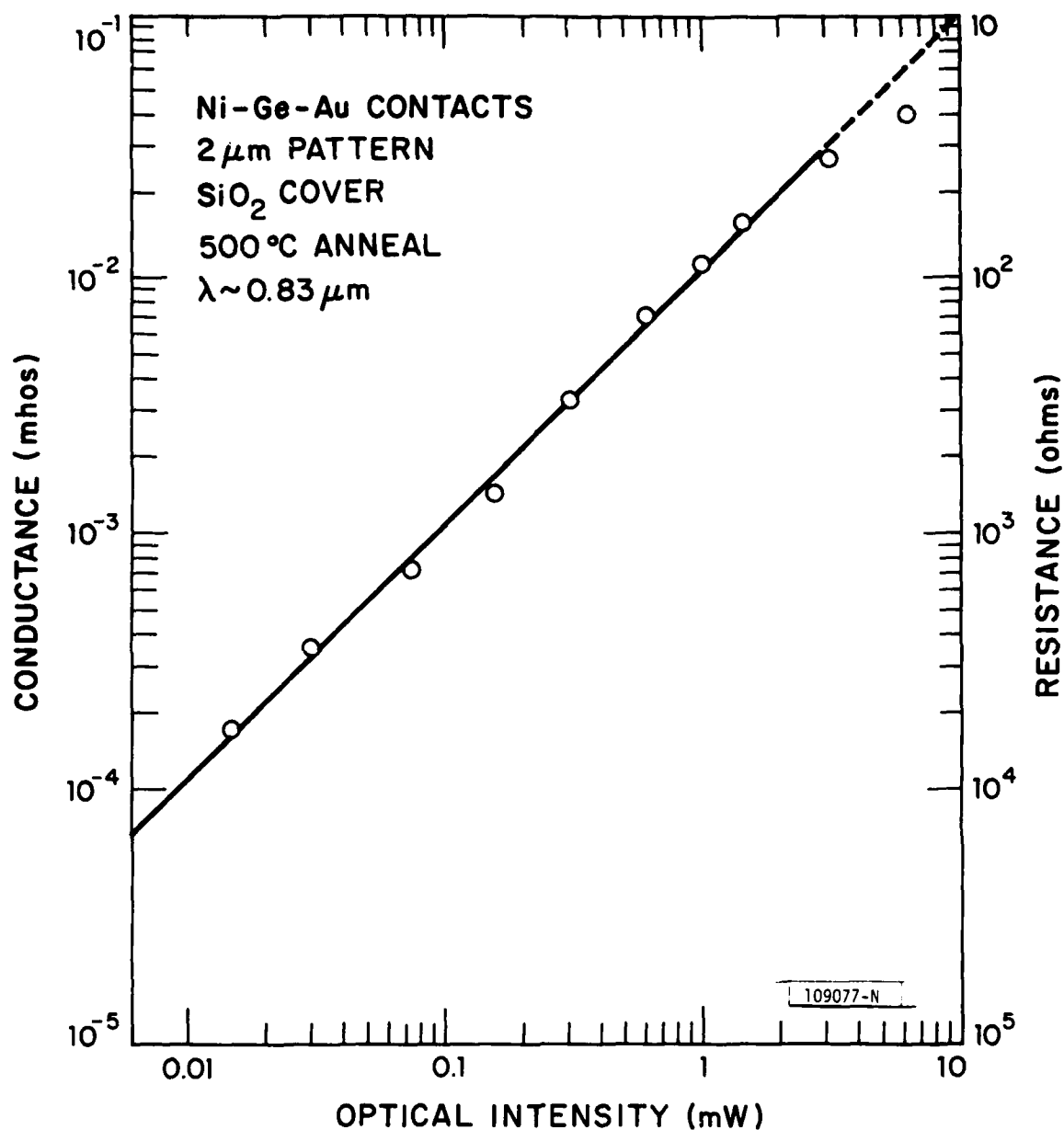


Fig. 5. On-state conductance vs incident optical power ($\lambda \sim 0.85 \mu\text{m}$) for an InP optoelectronic switch with NiGeAu contacts. This device had a 2- μm finger pattern, and was alloyed at 500°C with a SiO₂ cover.

where A is the area covered by the interdigitated pattern and \hat{C} is the capacitance of a finger pair per unit length. The RC time constant² calculated from this product is

$$RC = \frac{\hat{C}Ah\nu\ell}{4P\tau\mu e} \quad (5)$$

The frequency ω_c at which the magnitude of the impedances in the on and off states is the same is given by $\omega_c = (RC)^{-1}$. This frequency is maximized by making the optical intensity large, the mobility large, and the finger length small.

Noting that $\omega_m = \tau^{-1}$, we may rewrite Eq. (5):

$$\omega_c\omega_m = \frac{4P\mu e}{\hat{C}Ah\nu\ell} \quad (6)$$

When the switch is used as a mixer, ω_c sets the maximum RF input frequency while ω_m sets the maximum local-oscillator frequency with the LO injected optically in this device. The product of these two frequencies as given by Eq. (6) is a figure of merit which depends on only two material properties μ and \hat{C} .

As may be seen from Eqs. (1) and (5), both the on-state resistance and the device RC time constant² are minimized by large values of the photoconductive lifetime τ and carrier mobility μ . In fact, InP was chosen as the most suitable material for this program because of its large effective electron mobility in these photoconductive applications ($\mu \sim 2000 \text{ cm}^2/\text{V-sec}$) at photoconductive lifetime values in the 1-nsec-and-shorter range. However, it is also clear that the lifetime must be small enough to allow the device to follow the frequency variations for a particular application. The availability of a range of photoconductive lifetimes is clearly desirable. We have found that the lifetimes do vary in our experiments with the lifetime

dependent on the starting InP crystal. The photoconductive lifetime of the starting material is attractively short for many applications. Furthermore, an additional processing sequence which involves the use of proton bombardment and thermal anneal can be used to further shorten the lifetime.

The photoconductive response times were measured using the circuit shown in Fig. 6. A commercial low-threshold AlGaAs diode laser ($\lambda \sim 0.85 \mu\text{m}$) driven by a commercial impulse-train generator was used as a pulsed light source. The light pulses had a repetition rate of 100 MHz and a full width at half maximum (FWHM) of $\lesssim 100$ psec, as measured by an InP/GaInAsP/InP n^+-n-p^+ photodiode fabricated at Lincoln Laboratory. The peak optical power focussed on the device was estimated to be 3 mW. A dc voltage of 300 mV was applied to one side of the switch and the output observed on a 50- Ω sampling oscilloscope. For samples processed in standard fashion, the 90%-to-10% fall times of the photoconductive response ranged from 6 to 0.5 nsec, corresponding to lifetimes of 2.7 to 0.23 nsec. It will be assumed here that the photoconductive lifetime is equal to the carrier lifetime, a reasonable assumption in view of the very small RC time constant in this 50-ohm system with $C < 10^{-13}$ F. Figure 7 illustrates the response for a sample with a lifetime of ~ 0.55 nsec. In all cases, the measured values of lifetime and bulk electron mobility were consistent with the on-state resistance measured using the HeNe laser system.

If devices with still faster performance are needed, proton bombardment may be used to reduce the photoconductive fall times to less than 100 psec. The electron mobility in these bombarded devices can nevertheless be $> 600 \text{ cm}^2/\text{Vsec}$ (compared to $\sim 2000 \text{ cm}^2/\text{Vsec}$ for the unbombarded devices as noted above), over an order-of-magnitude larger than that of devices of comparable speed made on other high-resistivity materials. This relatively large

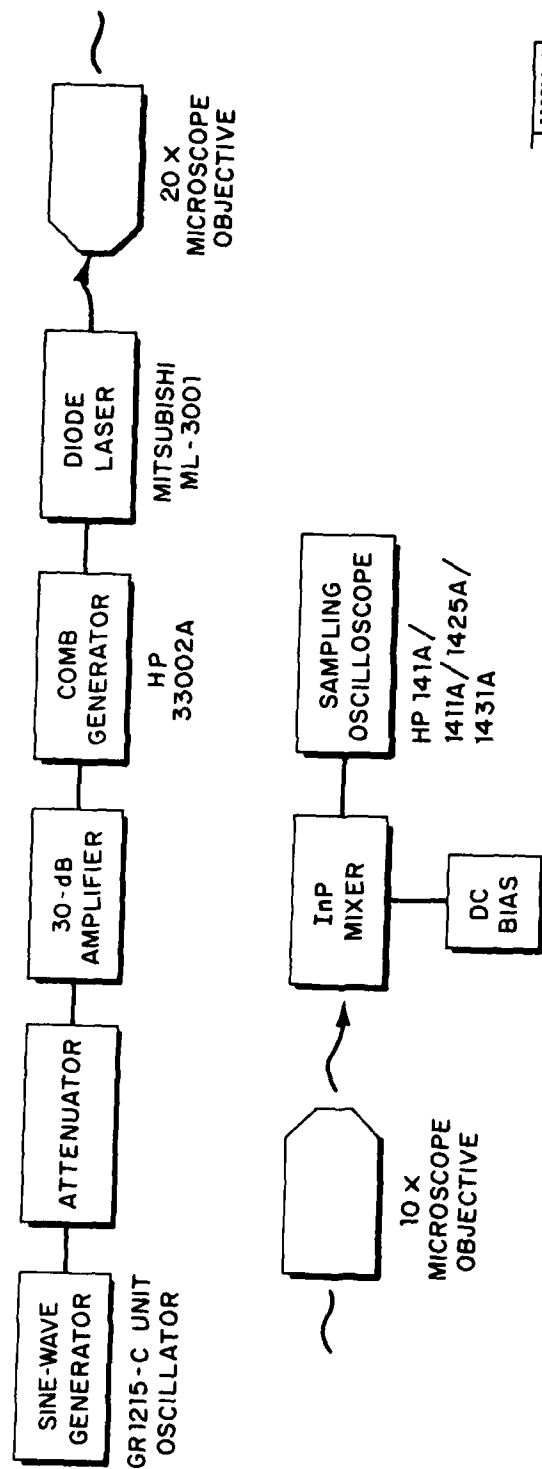


Fig. 6. Block diagram of the circuit used to measure the response time of InP optoelectronic switches. The width of the optical pulses is estimated to be ≤ 100 psec, full width at half maximum.

113718-N

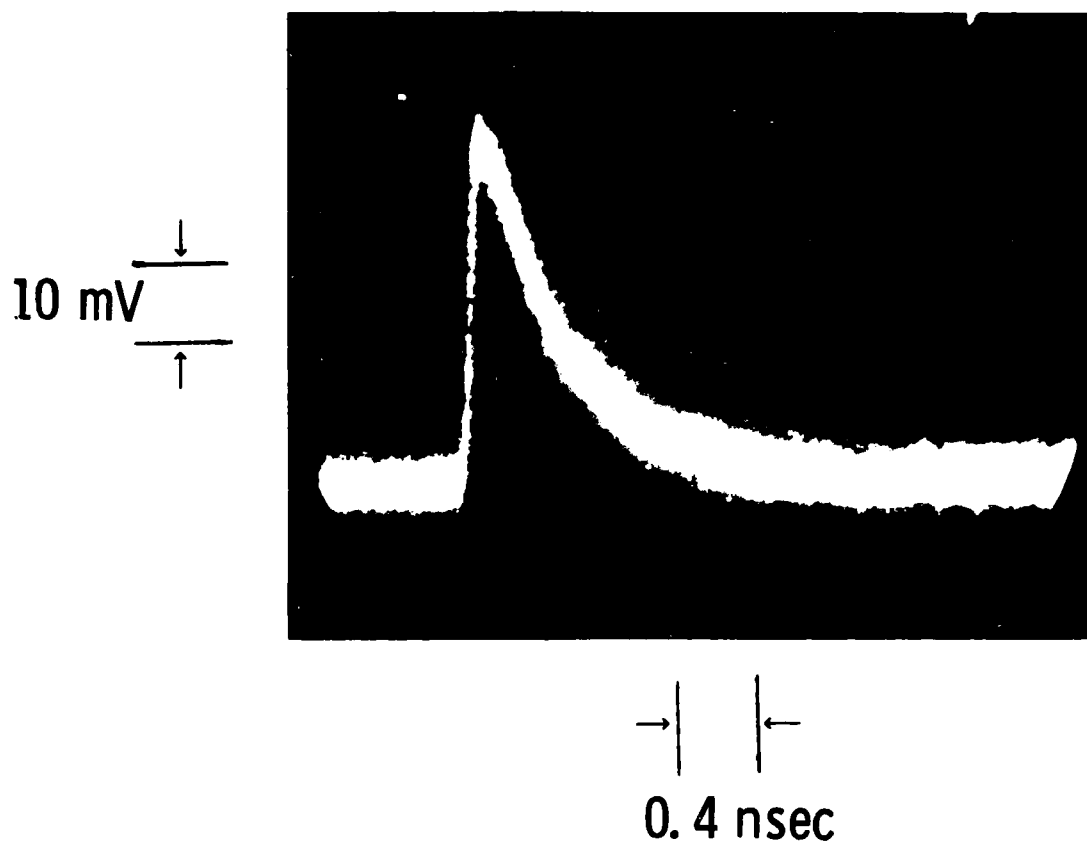


Fig. 7. Photoresponse of InP optoelectronic switch to short pulses (<100 psec) of AlGaAs diode-laser light ($\lambda \sim 0.85 \mu\text{m}$) of 3-mW peak power, as obtained with the circuit shown in Fig. 6. In this test, a dc voltage of 300 mV was connected between ground and one terminal of the device, with the response shown observed between the other terminal and ground on a high-speed sampling oscilloscope (response time ~ 25 psec, input impedance = 50Ω).

mobility implies that with similar structures and bias levels, the InP devices should have over an order-of-magnitude larger response for a given light level.

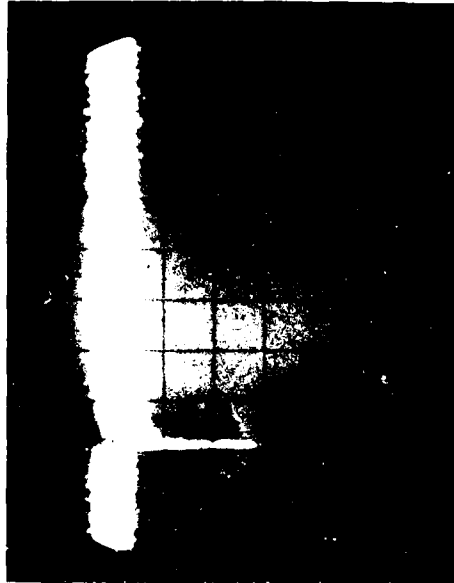
Two sets of experiments were done to investigate the effects of proton bombardment on the response of these InP optoelectronic devices, with a different schedule of bombardment used in each experiment. In the first set of experiments, the InP sample was prepared in standard fashion as described previously with the Au/Ge/Ni metalization technique and the 6-, 4- and 2- μm geometry device patterns. The sample was then cleaved into five separate pieces, with each piece having several devices of the 2- μm geometry. One piece was set aside as a standard, and the remaining four were bombarded with a $10^{13}/\text{cm}^2$ dose of 200-keV protons. Next, three of these samples were annealed in hydrogen, one at 250°C, one at 300°C, and one at 350°C, each for 10 sec. Each sample was then cemented to a grooved aluminum block and wire bonded to OSM connectors for evaluation.

Preliminary low-speed measurements were done by means of the raster-scanned He-Ne laser-light-spot technique to insure that these devices had the uniformity of photoresponse, linearity of current-voltage characteristics and the near-theoretical sensitivity of earlier devices.

The results of these tests of the effects of proton bombardment are shown in Figs. 8 and 9. For the unbombarded device, the decay of the photoresponse is approximately exponential with 90%-to-10% fall time of ~ 5 nsec (time constant of ~ 2.3 nsec). Also from the previous study of device resistance as a function of finger geometry, the electron mobility is estimated to be ~ 2000 cm^2/Vsec . Following bombardment, both the response time and mobility are substantially reduced, with the rise and fall times each < 100 psec and electron mobility of ~ 200 cm^2/Vsec . Following bombardment and



(a)



(b)

Fig. 8. Photoresponse of InP optoelectronic switch with the conditions outlined in Fig. 7: (a) Unbombarded device. (b) Device bombarded with a $10^{13}/\text{cm}^2$ dose of 200-keV protons and subsequently annealed at 250°C for 10 sec.

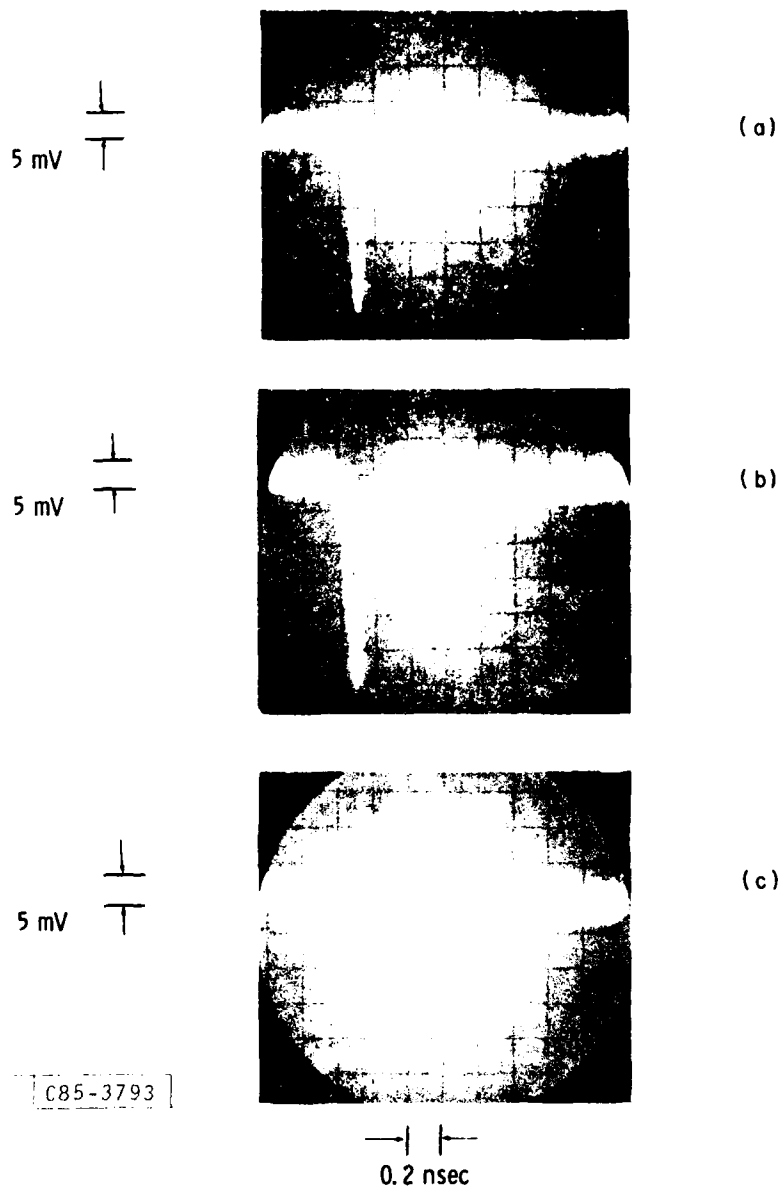


Fig. 9. Photoresponse of three InP optoelectronic switches, as described in Fig. 7, following proton bombardment and subsequent 10-sec anneal at: a. 250°C; b. 300°C; c. 350°C.

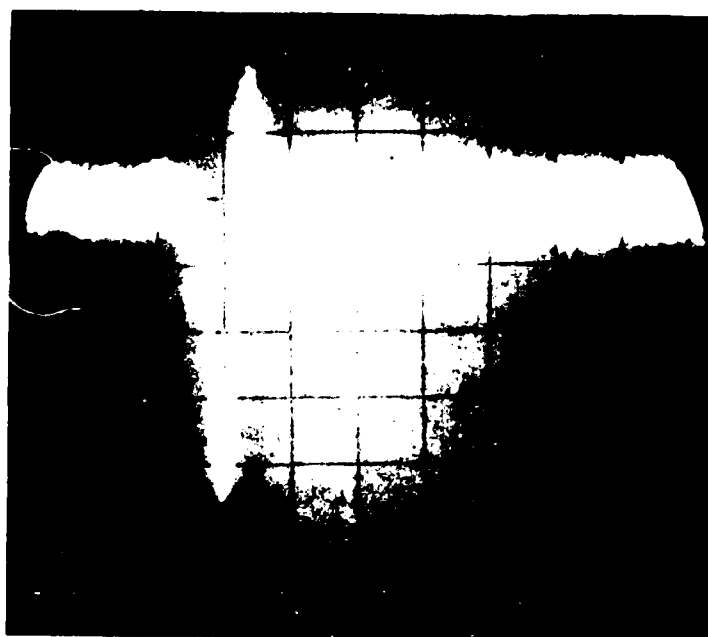

the 250°C anneal, the rise and fall times remained at <100 psec but the mobility recovered to at least 1000 cm²/Vsec. The mobility recovery was estimated by the amplitude of the photoresponse compared to that of the unbombarded device. It should be noted that this measurement may underestimate the mobility value in this case due to carrier recombination during the light pulse. Finally, with increasing anneal temperature, the rise and fall times remain at <100 psec, and the mobility remains at >1000 cm²/Vsec. However, the bombarded devices show a small "back porch" on the trailing edge of the response. This back-porch component increases in magnitude as the device is annealed toward its unbombarded state. The shape of these pulses was insensitive to focusing and total light incident on the device.

The samples for the second set of experiments were processed identically as those for the first set, except for the bombardment. In this case, a schedule of 10¹³/cm² protons at each of three energies, 100 keV, 200 keV, and 300 keV was used to provide a more nearly uniform depth distribution of bombardment effects. The results were similar to those of the first experiments, except for a substantially reduced "back porch". Figure 10 shows the response of the sample prepared in this way and annealed at 250°C for 10 sec. It is clear that the trailing edge is much sharper than that seen in Fig. 3(a) with a FWHM of 70 psec. However, package resonance effects limit our ability to interpret the trailing edge, and improved packages are in progress. As for the first experiment, the estimated mobility of >600 cm²/Vsec must be regarded as a lower limit due to carrier recombination during the light pulse.

Another effect of the bombardment that may be a limitation in some cases is a decrease in the off-state (dark) resistance. For the device of the second experiment that was bombarded and annealed at 250°C, the off-state

(35-3795)

5 mV



0.2 nsec




Fig. 10. Photoresponse of an InP optoelectronic switch as in Fig. 2(b), except that the dc voltage was 500 mV and the device was bombarded with $10^{13}/\text{cm}^2$ protons at 100 keV, 200 keV, and 300 keV, respectively, and subsequently annealed at 250°C for 10 sec.

resistance decreased from >10 Mohms to ~ 100 Kohms. This value can be compared with the peak on-state value of ~ 1000 ohms in the present pulsed experiment, and an anticipated value of <100 ohms when the laser is replaced with one having greater output power. However, the off-state resistance decrease may not be a necessary result of proton bombardment, and more work with different bombardment and anneal schedules, and perhaps with other ions, is needed to investigate this effect. Also since higher proton doses have been shown to increase absorption below the band edge, it may be possible to extend the wavelength sensitivity of these devices to $>1 \mu\text{m}$.

III. MIXER RESULTS

An initial investigation of the performance of these InP optoelectronic devices as mixers has been done with device operation in both a switch mode and also in a bilinear mode. In the switch mode, the device operates as an on-off multiplier, similar to the conventional diode-bridge mixers, whereas in the bilinear mode, the device output has a component that is linear in both inputs.

1. Switch Mode

The circuit of Fig. 11 was used to investigate operation in the switch mode. The InP optoelectronic mixer was illuminated with light from an AlGaAs diode laser (Hitachi) that was driven by a HP214A Pulse Generator at a 50% duty cycle, approximating a square wave drive. The rf input to the InP device was taken from a HP462A amplifier, which was in turn driven by two HP signal generators operating at slightly different frequencies near 1 MHz. The mixer output was fed directly into a HP Spectrum Analyzer. With this arrangement, the conventional mixer measurements of conversion loss and third-order, two-tone intermodulation product were done for a range of light intensities illuminating the mixer. A typical result is shown in Fig. 12.

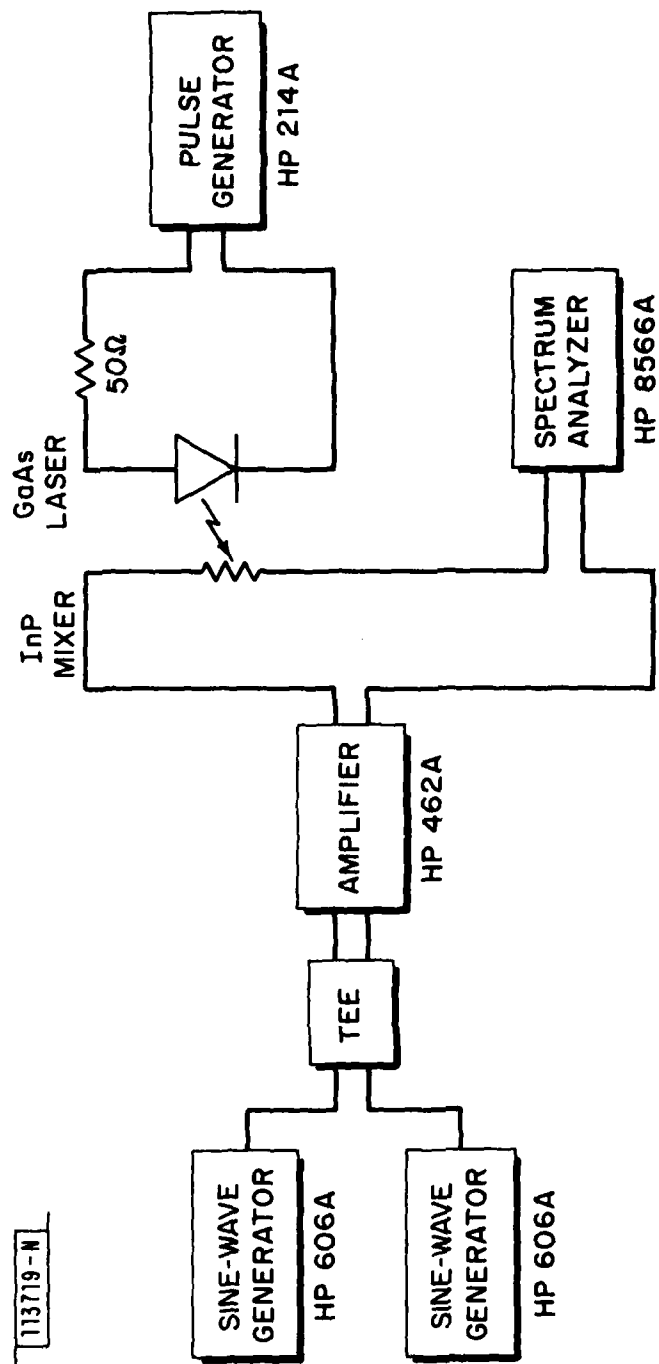


Fig. 11. Block diagram of the circuit used to evaluate the performance of InP optoelectronic mixers in the switch mode of operation.

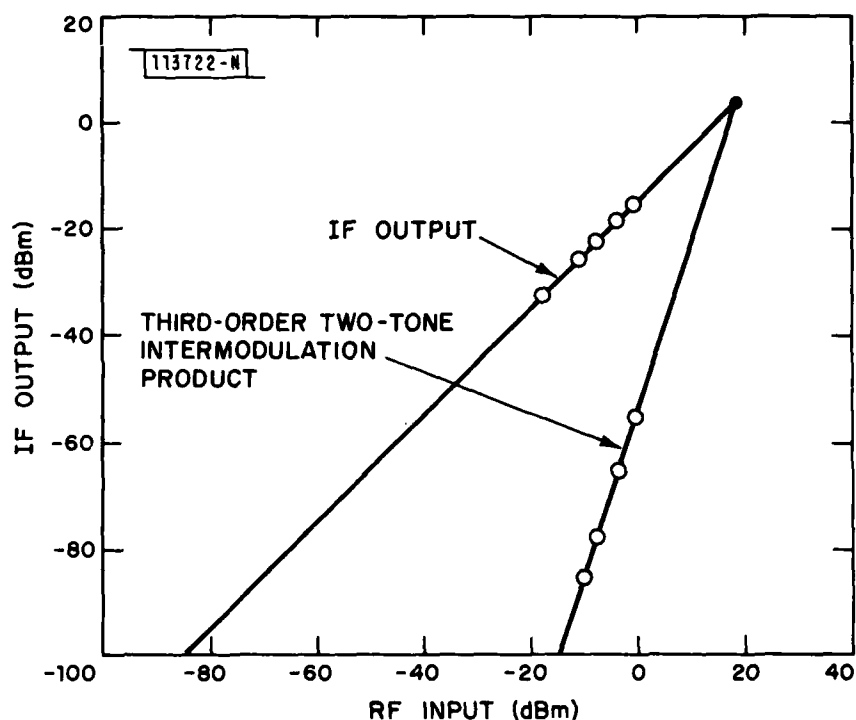


Fig. 12. I.F. output and third-order, two-tone intermodulation product of an InP optoelectronic mixer as a function of the r.f. input power in each of the two equal-input-level signals. The InP device had a 2- μ m-finger pattern and an on-state resistance of 21 ohms. The two r.f. input frequencies and the local oscillator frequency were 1.24, 1.1, and 1 MHz, respectively.

In this case, a device with a 2- μ m pattern was used, and the diode laser drive was adjusted to give a InP device on-state resistance of 21 ohms. Both the IF component and the third-order, two-tone component have the expected slopes of one and three, respectively. The insertion loss is ~15 dB, of which ~10 dB is due to the present mode of operation. Lower losses could be achieved by using multiple switches and balanced configurations, as is done with conventional mixers.

The third-order, two-tone intermodulation product value of -55 dBm at an rf input of ~0 dBm that was observed for the device on Fig. 12 is comparable to values seen for conventional diode-bridge mixers. However, by varying the on-state resistance of the InP mixer and measuring the IM product, it is possible to predict much better performance. The results of one such measurement are shown in Fig. 13, where the IM product is plotted as a function of device on-state conductance for several rf input power levels. The on-state conductance was varied by changing the light power incident on the InP mixer. As shown, the IM product (measured in dB) decreases with increasing device on-state conductance. Increasing the conductance is therefore beneficial in two ways: lower insertion loss and lower intermodulation product. Such an increase in on-state conductance could be obtained with increased laser power, smaller geometry devices, or lower intercept resistance. These approaches will be evaluated during the coming year.

2. Bilinear Mode

In addition to the switch mode of operation, it is possible to operate these InP mixers in a bilinear mode in which the output is a linear product of the two electrical inputs to the mixer. This mode of operation is made possible by the linearity of device conductance with light level, and by the linearity of diode laser output with input current. In the simplest circuit

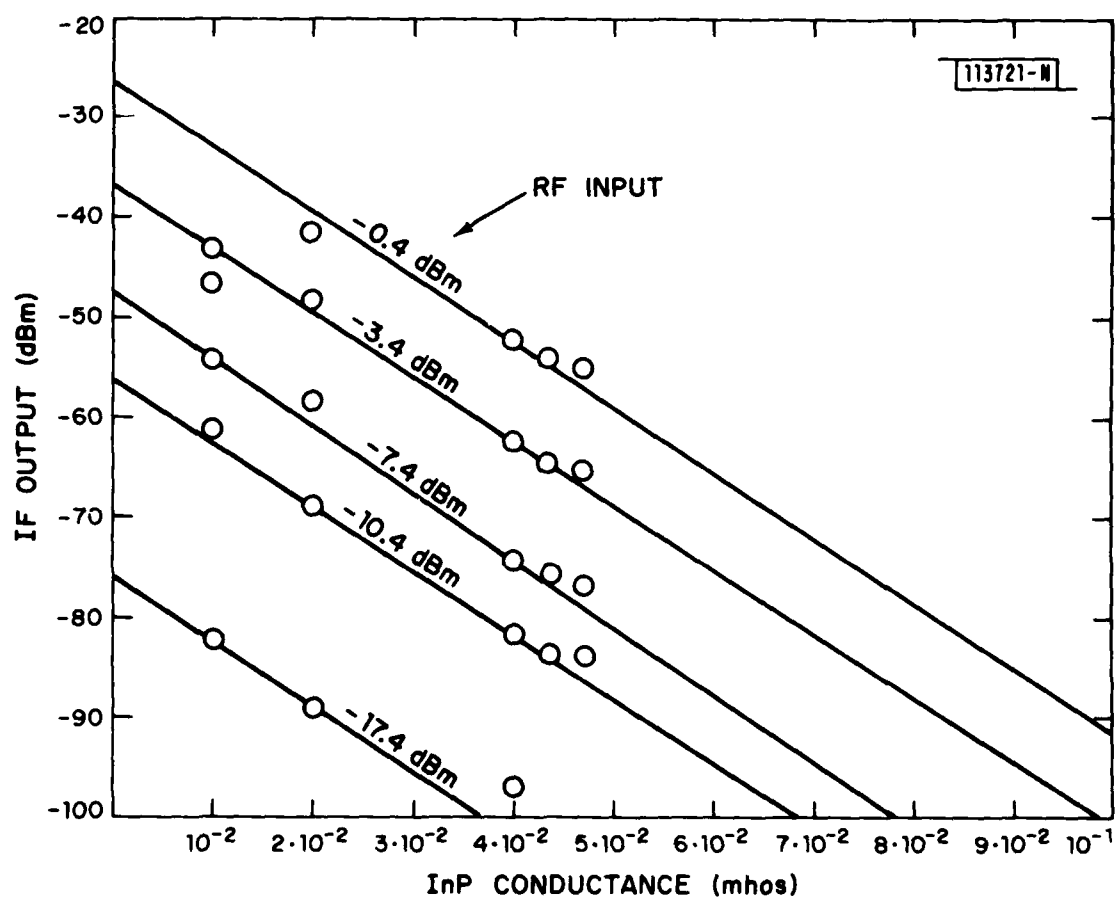


Fig. 13. Third-order, two-tone intermodulation (IM) product as a function of InP mixer on-state conductance for the device used in Fig. 12. The IM product is shown for a variety of r.f. input levels.

implementation of this mode, there is an additional term in the mixer output that is linear in the rf input to the mixer. However, the use of multiple devices and/or transformers to achieve a balanced configuration would eliminate this term.

The circuit that was used to investigate the bilinear mode of operation is shown in Fig. 14. This circuit is identical to the one of Fig. 11 except for the electrical input to the diode laser. In this case, the laser is dc biased so that 1 to 2 mW of laser power was focussed on the the InP mixer, and the ac input to the laser applied as a small signal to that dc level. Although the results shown in Fig. 15 are only preliminary, it is clear that linear operation in both inputs can be achieved.

In a separate experiment, in which the rf power was held fixed at -4.8 dBm, the IF output was linear with L.O. input over a 20-dB range.

IV. PROFESSIONAL PERSONNEL

The following individuals contributed to the research effort supported by this grant.

1. Arthur G. Foyt, Staff Member, Applied Physics Group
2. Frederick J. Leonberger, Assistant Group Leader, Applied Physics Group.
3. Richard C. Williamson, Group Leader, Applied Physics Group.

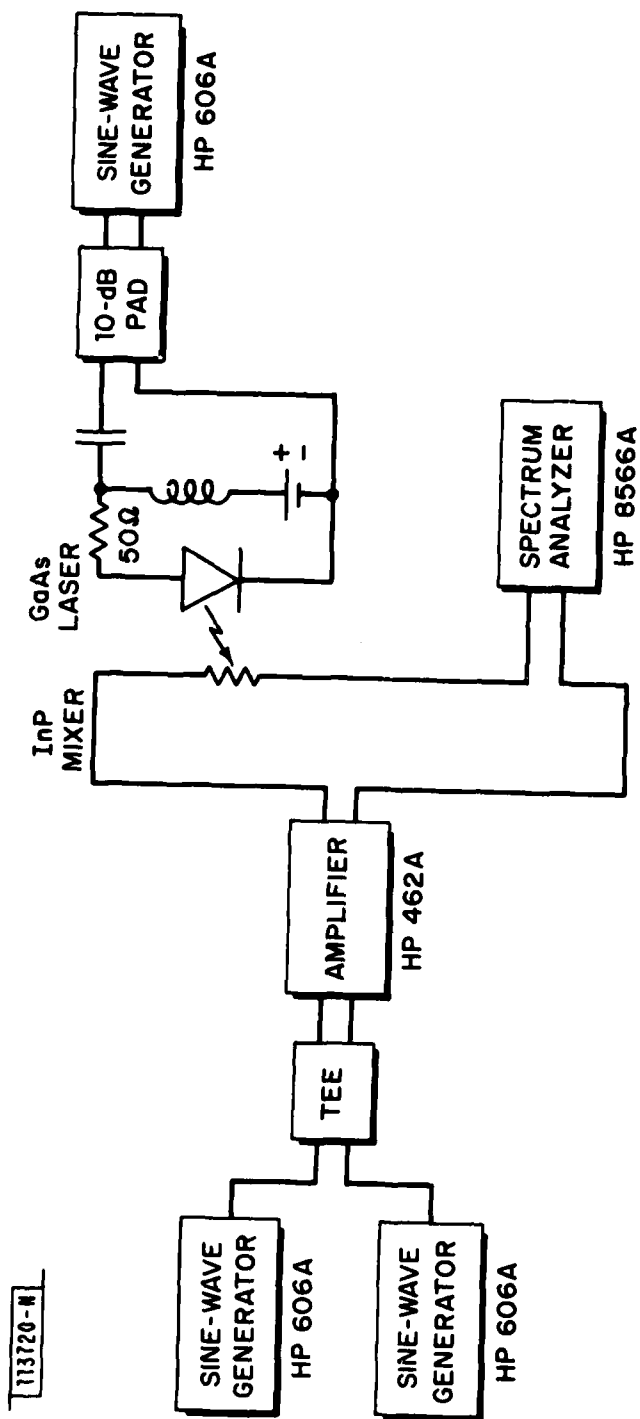


Fig. 14. Block diagram of the circuit used to evaluate the performance of InP optoelectronic mixers in the bilinear mode of operation.

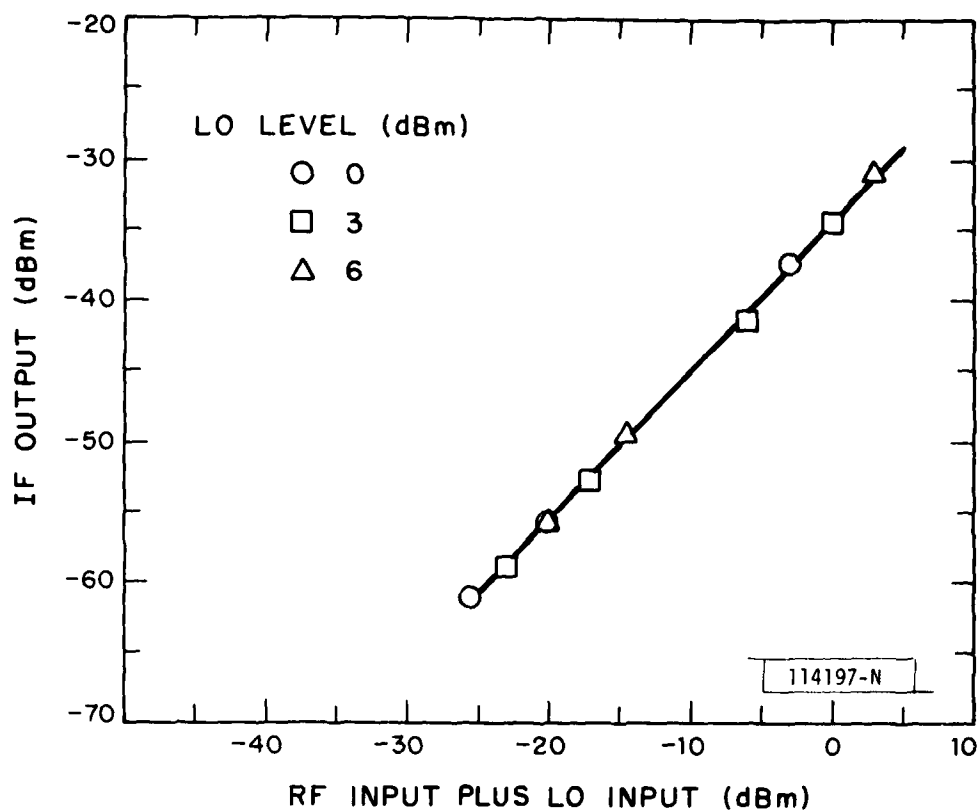


Fig. 15. I.F. output as a function of r.f. input level and L.O. input level for an InP optoelectronic mixer operating in the bilinear mode of operation. The device had a 2- μ m-finger pattern, and the d.c. light level was 2 mW. The r.f. and local-oscillator frequencies were 1.98 and 1.77 MHz, respectively.

UNCLASSIFIED

SECURITY CLASSIFICATION OF THIS PAGE (When Data Entered)

REPORT DOCUMENTATION PAGE		READ INSTRUCTIONS BEFORE COMPLETING FORM
1. REPORT NUMBER ESD-TR-82-008	2. GOVT ACCESSION NO. AD-A114 149	3. RECIPIENT'S CATALOG NUMBER
4. TITLE (and Subtitle) Acoustooptic Time-Integrating Correlators and Optoelectronic Mixers		5. TYPE OF REPORT & PERIOD COVERED Annual Report 1 February 1981 - 31 January 1982
		6. PERFORMING ORG. REPORT NUMBER None
7. AUTHOR(s) Arthur G. Foyt and Richard C. Williamson		8. CONTRACT OR GRANT NUMBER(s) F19628-80-C-0002
9. PERFORMING ORGANIZATION NAME AND ADDRESS Lincoln Laboratory, M.I.T. P.O. Box 73 Lexington, MA 02173-0073		10. PROGRAM ELEMENT, PROJECT, TASK AREA & WORK UNIT NUMBERS Program Element No. 61102F Project No. 2300
11. CONTROLLING OFFICE NAME AND ADDRESS Air Force Office of Scientific Research Bolling AFB, DC 20332		12. REPORT DATE 31 January 1982
		13. NUMBER OF PAGES 36
14. MONITORING AGENCY NAME & ADDRESS (if different from Controlling Office) Electronic Systems Division Hanscom AFB, MA 01731		15. SECURITY CLASS. (of this report) Unclassified
		15a. DECLASSIFICATION DOWNGRADING SCHEDULE
16. DISTRIBUTION STATEMENT (of this Report) Approved for public release; distribution unlimited.		
17. DISTRIBUTION STATEMENT (of the abstract entered in Block 20, if different from Report)		
18. SUPPLEMENTARY NOTES None		
19. KEY WORDS (Continue on reverse side if necessary and identify by block number) <div style="display: flex; justify-content: space-between;"> <div> optoelectronic mixer bilinear mixer correlator </div> <div> InP optoelectronic switch time-integrating correlator </div> </div>		
20. ABSTRACT (Continue on reverse side if necessary and identify by block number) <p>Research during the past year has been concentrated on the development of the InP optoelectronic switch and on the evaluation of this switch as an electronic mixer. This type of mixer appears well suited for use in a time-integrating correlator which employs a heterodyne detector array. In such an array, a small high-quality mixer is crucial.</p> <p>InP optoelectronic switches have been fabricated using interdigitated-finger electrode structures with finger and space lengths varying from 6 μm for the most widely spaced device to 1.25 μm for the most closely spaced device and active areas of 48 \times 48 μm. Devices fabricated using alloyed Au/Ge/Ni contacts have shown near-theoretical conductance when illuminated with laser light from either a He-Ne laser ($\lambda \sim 0.63 \mu\text{m}$) or from a AlGaAs laser ($\lambda \sim 0.84 \mu\text{m}$). For a device with 1.25-μm lines and spaces and with</p>		

UNCLASSIFIED

SECURITY CLASSIFICATION OF THIS PAGE (When Data Entered)

UNCLASSIFIED

SECURITY CLASSIFICATION OF THIS PAGE (When Data Entered)

20. ABSTRACT (Continued)

a 3-nsec photoconductor response fall time, an on-state (illuminated) resistance value of <18 ohms was measured using 6 mW of AlGaAs diode laser light power. Also, these devices exhibit a linear variation of on-state conductance with laser intensity from low light levels to levels greater than 2 mW. Such linear variation is essential for the operation of the device as a bilinear mixer. Finally, it has been found that the response times of these devices are somewhat dependent on the starting material, with the photoresponse fall times (90% to 10% of peak response) varying from ~6 nsec to 0.5 nsec. Also, it has been shown that proton bombardment can dramatically reduce the response time with only a modest change in the amplitude of the response. The 90%-to-10% fall time of a device with an initial fall time of 5 nsec was reduced to ~100 psec following a 200-kV $10^{13}/\text{cm}^2$ proton bombardment and subsequent anneal at 250°C, with the amplitude of the response decreased by only a factor of two. These InP structures have substantially higher carrier mobility (by over an order of magnitude) than similar amorphous Si, Silicon-on-Sapphire, or Ge structures of comparable speed.

The performance of these devices in both the conventional (switch) mode and the bilinear mode of mixing has been evaluated. For a structure with 2- μm lines and spaces and a photoresponse fall time of ~3 nsec, illumination with ~5 mW of AlGaAs laser power resulted in an on-state resistance of 21 ohms. For this device operating in the switch mode at 1 MHz, the third-order two-tone intermodulation products were -55 dBm for ~0 dBm of rf input power. A simple extrapolation suggests that these products could be lowered to -85 dBm at the same rf power level by reducing the on-state resistance by one-half which reduction should be possible to do by reducing the finger and space dimension, by reducing the intercept resistance, or by increasing the laser power. In a preliminary investigation of the bilinear mode of operation at 1 MHz, the multiplied output varied linearly with the rf input to the switch over a 20-dB range and with the input to the diode laser, also over at least a 20-dB range.

UNCLASSIFIED

SECURITY CLASSIFICATION OF THIS PAGE (When Data Entered)